Electrochemistry

Deutsche Ausgabe: DOI: 10.1002/ange.201501443
Internationale Ausgabe: DOI: 10.1002/anie.201501443

Radical Compatibility with Nonaqueous Electrolytes and Its Impact on an All-Organic Redox Flow Battery**

Xiaoliang Wei, Wu Xu, Jinhua Huang, Lu Zhang, Eric Walter, Chad Lawrence, M. Vijayakumar, Wesley A. Henderson, Tianbiao Liu, Lelia Cosimbescu, Bin Li, Vincent Sprenkle, and Wei Wang**

Abstract: *Nonaqueous redox flow batteries hold the promise of achieving higher energy density because of the broader voltage window than aqueous systems, but their current performance is limited by low redox material concentration, cell efficiency, cycling stability, and current density. We report a new nonaqueous all-organic flow battery based on high concentrations of redox materials, which shows significant, comprehensive improvement in flow battery performance. A mechanistic electron spin resonance study reveals that the choice of supporting electrolytes greatly affects the chemical stability of the charged radical species especially the negative side radical anion, which dominates the cycling stability of these flow cells. This finding not only increases our fundamental understanding of performance degradation in flow batteries using radical-based redox species, but also offers insights toward rational electrolyte optimization for improving the cycling stability of these flow batteries.*

The redox flow battery (RFB) has recently attracted a great deal of interest as a safe and cost-effective energy storage technology for power grid applications.[1] By storing dissolved electroactive materials in external tanks, the RFB decouples the energy and the power thus gaining tremendous design flexibility to meet different energy-to-power ratio (E/P) applications. Conventional aqueous RFBs are generally low-energy systems limited mainly by the narrow electrochemical stability window of water.[2] Although the energy density is generally not considered as a critical performance criterion for stationary applications, the low energy density of aqueous RFBs has nevertheless disqualified them from other energy storage markets. Therefore, recent efforts have shifted to developing nonaqueous RFBs (NRFBs) because of their potential high energy density due to the wider electrochemical window of nonaqueous electrolytes.[3] Current NRFB research is primarily focused on seeking viable redox materials for various flow chemistries, for example, metal coordination compounds[4] and organic redox molecules.[5]

The potential to achieve improved energy density has been demonstrated in some NRFB systems.[6] However, many other NRFBs suffer from insufficient energy densities primarily due to low concentrations of redox materials.[4a,5a] A second major limitation of the current NRFBs is the abysmal current densities, typically in the range of 0.01–0.5 mA cm^{-2}.[4a,5b] Apart from the low conductivity of nonaqueous electrolytes compared to aqueous counterparts, the ion-exchange membranes used in the previous reports are believed to be the other significant contributing factor to the low current density. Furthermore, the often observed irreversible capacity loss and limited cycling stability has been revealed as another major technical hurdle.[7] Unfortunately, there remains a critical knowledge gap in the fundamental understanding of capacity loss mechanisms in many NRFB systems.

Here we report a new nonaqueous all-organic flow chemistry along with a mechanistic study to elucidate the capacity fading mechanism. All-organic flow batteries capitalize on the advantages of structural diversity,[8] solubility tunability,[9] natural abundance, and environmental friendliness of organic materials. In this study, 9-fluorenone (FL) and 2,5-di-*tert*-butyl-1-methoxy-4-[2′-methoxyethoxy]benzene (DBMMB) were chosen as the anolyte and the catholyte redox materials (denoted as FL|DBMMB), respectively, because of their high solubility in various solvents and well-defined electrochemistries. DBMMB analogs have been explored as redox shuttle additives for overcharge protection in Li-ion batteries and as redox materials for NRFBs.[10] The redox reactions are illustrated in Scheme 1. Instead of using an ion exchange membrane, we adopted a microporous separator to enable the high current operation (30 times increase) of the NRFB, due to the unique open pore structure and large ionic transport channels in the porous separator

[*] Dr. X. Wei, Dr. W. Xu, Dr. E. Walter, Dr. C. Lawrence, Dr. M. Vijayakumar, Dr. W. A. Henderson, Dr. T. Liu, Dr. L. Cosimbescu, Dr. B. Li, Dr. V. Sprenkle, Dr. W. Wang
Pacific Northwest National Laboratory
902 Battelle Blvd, Richland, WA 99352 (USA)
E-mail: Xiaoliang.Wei@pnnl.gov
Wei.Wang@pnnl.gov
Dr. J. Huang, Dr. L. Zhang
Argonne National Laboratory
9700 South Cass Avenue, Argonne, IL 60439 (USA)
Dr. X. Wei, Dr. J. Huang, Dr. L. Zhang, Dr. W. Wang
Joint Center for Energy Storage Research (JCESR; USA)

[**] This research was financially supported by the U.S. Department of Energy's (DOE's) Office of Electricity Delivery and Energy Reliability (OE) under contract number 57558 (flow chemistry development and electrochemical tests); by the Joint Center for Energy Storage Research (JCESR), an Energy Innovation Hub funded by the U.S. Department of Energy, Office of Science, Basic Energy Sciences (synthesis of DBMMB); and by the William R. Wiley Environmental Molecular Sciences Laboratory (EMSL), a national scientific user facility sponsored by DOE's Office of Biological and Environmental Research, under proposal numbers 48374 and 48293 (ESR measurements). PNNL is a multi-program national laboratory operated by Battelle for DOE under contract number DE-AC05-76L01830.

Supporting information for this article is available on the WWW under http://dx.doi.org/10.1002/anie.201501443.

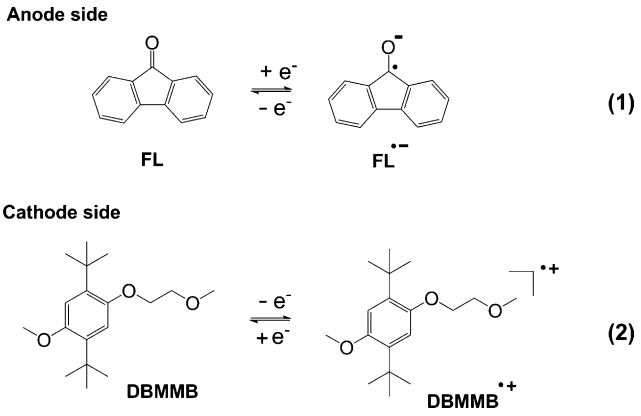

Scheme 1. Redox reactions of the nonaqueous FL | DBMMB flow battery.

allowing high ionic conductivity.[11] Meanwhile, a mixed-reactant electrolyte design was adopted in order to mitigate the crossover of the active species.[12]

A high electrolyte conductivity is always favored in RFBs and is critically important for achieving high power capability and cycling efficiency. Suitable supporting electrolytes with high ionic conductivities therefore need to be identified. As shown in Figure S1 in the Supporting Information, electrolytes containing acetonitrile (MeCN) and tetraethylammonium (TEA^+)-based salts have considerably higher conductivities than other electrolytes studied and thus were initially used in the FL | DBMMB chemistry. To determine the redox potentials, cyclic voltammetry (CV) was performed in a mixed-reactant electrolyte of tetraethylammonium bis(trifluoromethylsulfonyl)imide (TEA-TFSI)/MeCN containing a 1:1 molar ratio of FL:DBMMB. As shown in Figure 1a, FL and DBMMB show redox potentials at −1.64 V and 0.73 V versus Ag/Ag^+ (10 mM), respectively, resulting in a cell voltage of 2.37 V for the FL | DBMMB flow chemistry. FL has a high solubility of 2.0 M in MeCN and DBMMB (liquid at room temperature) is highly miscible with MeCN. In the mixed-reactant electrolyte, the solubility limit for both redox materials is 0.9 M in 1.2 M TEA-TFSI in MeCN.

Figure 1b shows the cycling efficiency and capacity of a FL | DBMMB flow cell using a redox electrolyte of 0.5 M FL/0.5 M DBMMB/1.0 M TEA-TFSI/MeCN, and Figure S2 shows the typical cycling voltage curves of this flow cell. The area specific resistivity (ASR) of the flow cell was 23.2 $\Omega\,cm^2$, which allowed the flow cell to cycle at a current density of 15 $mA\,cm^{-2}$ while still having relatively high efficiencies, that is, coulombic efficiency (CE) of 86%, voltaic efficiency (VE) of 83%, and energy efficiency (EE) of 71%. Such a high current density was made possible by the reduced flow cell resistance which was achieved through the uses of the high-conductivity supporting electrolyte and the porous separator. Accordingly, the flow cell demonstrated a high utilization ratio of about 87% of the redox materials, as indicated by the first cycle charge capacity (5.8 $Ah\,L^{-1}$) versus the theoretical capacity (6.7 $Ah\,L^{-1}$). This flow cell exhibits an energy density of 15 $Wh\,L^{-1}$ during charge and 11 $Wh\,L^{-1}$ during discharge. Such an energy density, cell efficiency, and operational

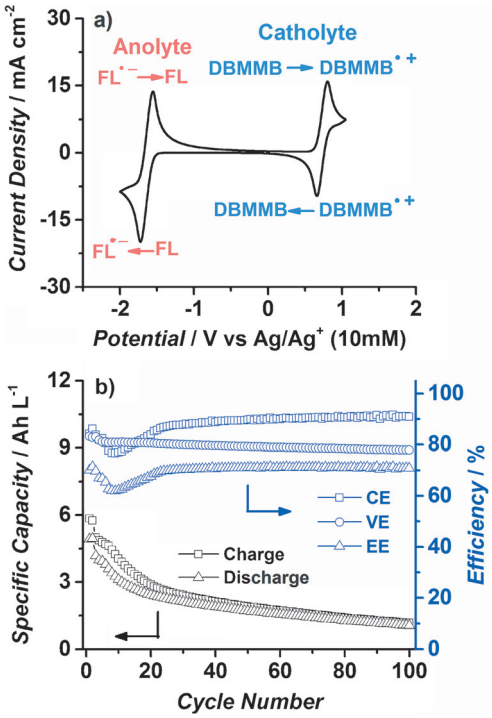

Figure 1. a) CV curve of 0.1 M FL/0.1 M DBMMB/1.0 M TEA-TFSI/MeCN at a voltage sweeping rate of 50 $mV\,s^{-1}$. b) Cycling efficiency and capacity of the FL | DBMMB flow cell using 0.5 M FL/0.5 M DBMMB/1.0 M TEA-TFSI/MeCN at 15 $mA\,cm^{-2}$.

current density are significantly higher than those for other all-organic NRFBs which delivered low energy densities, for example, about 2 $Wh\,L^{-1}$, or operating at limited current densities, for example, smaller than or equal to 0.35 $mA\,cm^{-2}$.[5] However, the FL | DMBBM flow system failed to produce stable cycling (Figure 1b). The CE and EE suffer from quick drops during the first 10 cycles, although gradual increases are observed afterwards. The charge capacity constantly fades from 5.8 to 1.2 $Ah\,L^{-1}$ over the 100 cycles, losing 80% of its original value. This limited cycling stability inevitably impairs the reliability of the FL | DBMMB flow chemistry.

As shown in Scheme 1, both redox reactions involve free radical ions, that is, the $FL^{\bullet-}$ radical anion at the anode side and the $DBMMB^{\bullet+}$ radical cation at the cathode side. Because radicals are usually chemically reactive, their chemical stability in the supporting electrolyte may conceivably impact the cycling stability of the flow cell. To gain insight into the validity of this hypothesis, an electron spin resonance (ESR) study was performed to elucidate the chemical stability of the two radicals in the tested TEA-TFSI/MeCN electrolyte and several other solvents and salts. TEA-BF_4, TEA-TFSI, and LiTFSI were selected to test the effects of different salt anions and cations. 1,2-Dimethoxyethane (DME) was selected to test the solvent effect due to its relatively high stability against radicals.[13] Figure 2a and b shows the fading of the ESR integrals (i.e. the radical concentrations) of the $FL^{\bullet-}$ and $DBMMB^{\bullet+}$ radicals as a function of storage time, indicating that the solvents and salts indeed have a significant effect on the lifetime of these two radicals, especially the $FL^{\bullet-}$.

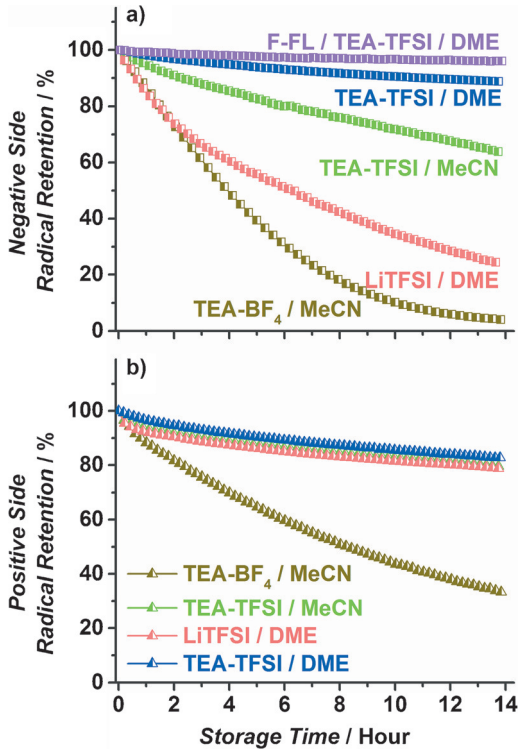

Figure 2. ESR measured radical fading in various supporting electrolytes: a) negative side ($FL^{\bullet-}$) and b) positive side ($DBMMB^{\bullet+}$). The experiment using 2-fluoro-9-fluorenone (F-FL) was used to demonstrate the proposed capacity decay mechanism, which is closely related with radical stability, in later paragraphs.

The $DBMMB^{\bullet+}$ shows much slower fading rates than the $FL^{\bullet-}$ in all of these supporting electrolytes, indicating the lower chemical stability of $FL^{\bullet-}$. In addition, the $FL^{\bullet-}$ is much more sensitive to the supporting electrolyte than the $DBMMB^{\bullet+}$; the latter shows a comparably marked chemical stability in all of these media except where the BF_4^- salt anion was used. With the same TEA-TFSI salt, the $FL^{\bullet-}$ is considerably more chemically stable in the DME solvent than in MeCN. With the same DME solvent and $TFSI^-$ salt anion, the TEA^+ cation leads to much better chemical stability for $FL^{\bullet-}$ than Li^+. With the same MeCN solvent and TEA^+ salt cation, both radicals are much more persistent with the $TFSI^-$ salt anion than BF_4^-.

The ESR result indicates that degradation of the $FL^{\bullet-}$ is closely associated with the nature of solvents and salts. The faster fading in MeCN than in DME may originate from depletion of the $FL^{\bullet-}$ by side reactions with MeCN through either nucleophilic substitution at the cyano C atom or proton extraction at the methyl group [Equations (1) and (2) in Scheme 2].[14] The BF_4^- salt anion causes quick fading for both $FL^{\bullet-}$ and $DBMMB^{\bullet+}$ owing to its high reactivity with these radicals.[15] There is another possibility as well. As a type of ketyl radical anions, the $FL^{\bullet-}$, although already stabilized by the two aromatic rings by conjugation, may still react with a second $FL^{\bullet-}$ to form dimeric FL_2^{2-} following the pinacol coupling pathway [Eq. (3) in Scheme 2].[16] This may explain why the TEA^+ results in slower radical fading than Li^+ in the same DME solvent. Specifically, while poorly coordinating to

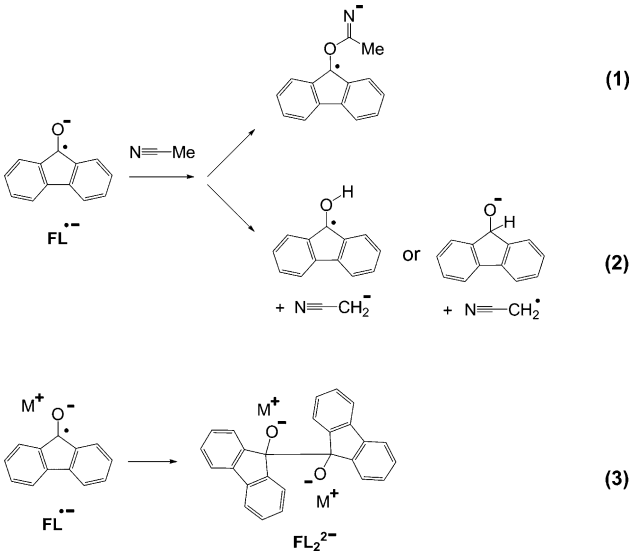

Scheme 2. Possible degradation mechanisms of the $FL^{\bullet-}$ radical anion.

the oxygen atom in the $FL^{\bullet-}$, the close proximity of the bulky TEA^+ cations may largely block a second $FL^{\bullet-}$ approaching the shielded reaction site, that is, the unpaired electron on the carbon atom.

The radical compatibility study derived from ESR provides a design guideline to achieve performance improvement for the FL|DBMMB flow battery by electrolyte optimization. The optimal supporting electrolyte among all those tested in ESR should be the TEA-TFSI/DME electrolyte which offers the best chemical stability for both radicals. This is proven by flow cell tests in these different supporting electrolytes (Figure 3a), which demonstrate that the flow cell using TEA-TFSI/DME maintained 90% of its original capacity over 50 cycles, a much higher value than for the other electrolytes. The capacity retention of these flow cells is in fair accord with their CE (Figure 3b) which reflects the amount of corresponding side reactions, considering the same cell cycling conditions resulting in a similar extent of crossover for all the electrolyte cases. In addition, the trend of the $FL^{\bullet-}$ fading matches well with the capacity fading in flow cells, indicating that the chemical instability of the $FL^{\bullet-}$ is the major contributor to the capacity fading in flow cells. This argument is supported by the fact that the flow cell using 2-fluoro-9-fluorenone (F-FL) produces even slower $F\text{-}FL^{\bullet-}$ fading and better capacity retention (Figure 2a and Figure 3a), which is attributed to the electron withdrawing -F group further delocalizing the unpaired electron thus improving the radical stability. This result also suggests that rational structural tailoring of redox materials is important for improving the chemical durability of redox species thus cycling stability of flow cells.

In conclusion, we have developed a new nonaqueous all-organic RFB based on high concentrations of FL and DBMMB with a cell voltage larger than 2 V. Although an EE larger than 70% and a current density larger than 10 mA cm^{-2} can be achieved, the cycling stability of the flow cells is limited. The ESR result clearly demonstrates that both solvents and salts strikingly affect the chemical stability of the

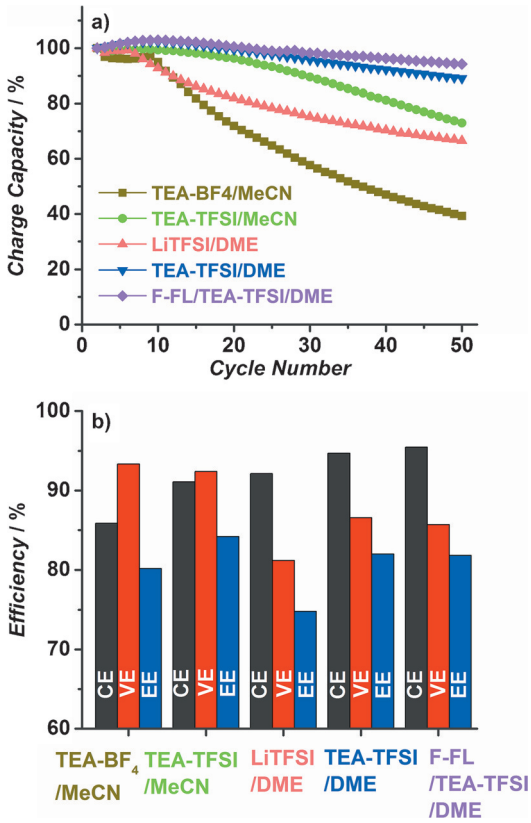

Figure 3. Effects of different solvents and salts on the cycling performance of flow cells using 0.1 M FL/0.1 M DBMMB/1.0 M salt at 10 mA cm^{-2}: a) charge capacity retention and b) CE, VE, and EE. (The voltage curves of these flow cell tests shown in Figure S3 indicate the supporting electrolytes are also able to tune the cell voltage and overpotential.)

charged radical species, especially the FL$^{\bullet-}$. This study not only reveals the capacity fading mechanism in the FL|DBMMB flow cells, but also directs the pathway to optimizing the supporting electrolyte for the FL|DBMMB flow battery. The TEA-TFSI/DME electrolyte, which offers the highest chemical stability to both radicals, is proven to be the best supporting electrolyte among those studied. This is primarily attributable to the high stabilities of both DME and TEA-TFSI against radical species and possibly the steric hindrance to dimerization offered by the bulky TEA$^+$. In addition, we also demonstrated that structure modification of the organic redox species can substantially improve their stability in the supporting electrolyte, and thus the flow cell performance. Although further improvement may still be necessary to make the FL|DBMMB flow chemistry suitable for practical applications, this study provides valuable insight for understanding the origin of performance degradation in flow cells involving organic radical-based redox species. This knowledge therefore serves as an important guidance for the selection and design of stable redox electrolyte systems for developing promising nonaqueous redox flow chemistries.

Keywords: electrochemistry · electrolyte optimization · ESR spectroscopy · nonaqueous redox flow batteries · radicals

How to cite: *Angew. Chem. Int. Ed.* **2015**, *54*, 8684–8687
Angew. Chem. **2015**, *127*, 8808–8811

[1] a) Z. G. Yang, J. Zhang, M. C. W. Kintner-Meyer, X. Lu, D. Choi, J. P. Lemmon, J. Liu, *Chem. Rev.* **2011**, *111*, 3577–3613; b) B. Dunn, H. Kamath, J. M. Tarascon, *Science* **2011**, *334*, 928–935.
[2] a) P. Leung, X. Li, C. P. de Leon, L. Berlouis, C. T. J. Low, F. C. Walsh, *RSC Adv.* **2012**, *2*, 10125–10156; b) M. Skyllas-Kazacos, M. H. Chakrabarti, S. A. Hajimolana, F. S. Mjalli, M. Saleem, *J. Electrochem. Soc.* **2011**, *158*, R55–R79.
[3] W. Wang, Q. Luo, B. Li, X. Wei, L. Li, Z. G. Yang, *Adv. Funct. Mater.* **2013**, *23*, 970–986.
[4] a) Q. Liu, A. E. S. Sleightholme, A. A. Shinkle, Y. Li, L. T. Thompson, *Electrochem. Commun.* **2009**, *11*, 2312–2315; b) P. J. Cappillino, H. D. Pratt, N. S. Hudak, N. C. Tomson, T. M. Anderson, M. R. Anstey, *Adv. Energy Mater.* **2014**, DOI: 10.1002/aenm.201300566.
[5] a) F. R. Brushett, J. T. Vaughey, A. N. Jansen, *Adv. Energy Mater.* **2012**, *2*, 1390–1396; b) Z. Li, S. Li, S. Liu, K. Huang, D. Fang, F. Wang, S. Peng, *Electrochem. Solid-State Lett.* **2011**, *14*, A171–A173.
[6] a) X. Wei, W. Xu, M. Vijayakumar, L. Cosimbescu, T. Liu, V. Sprenkle, W. Wang, *Adv. Mater.* **2014**, *26*, 7649–7653; b) Y. Zhao, H. R. Byon, *Adv. Energy Mater.* **2013**, *3*, 1630–1635; c) M. Duduta, B. Ho, V. C. Wood, P. Limthongkul, V. E. Brunini, W. C. Carter, Y. M. Chiang, *Adv. Energy Mater.* **2011**, *1*, 511–516.
[7] J. Mun, M. J. Lee, J. W. Park, D. J. Oh, D. Y. Lee, S. G. Doo, *Electrochem. Solid-State Lett.* **2012**, *15*, A80–A82.
[8] Z. P. Song, H. S. Zhou, *Energy Environ. Sci.* **2013**, *6*, 2280–2301.
[9] a) B. Huskinson, M. P. Marshak, C. Suh, S. Er, M. R. Gerhardt, C. J. Galvin, X. Chen, A. Aspuru-Guzik, R. G. Gordon, M. J. Aziz, *Nature* **2014**, *505*, 195–198; b) X. Wei, L. Cosimbescu, W. Xu, J. Hu, M. Vijayakumar, J. Feng, M. Y. Hu, X. Deng, J. Xiao, J. Liu, V. Sprenkle, W. Wang, *Adv. Energy Mater.* **2015**, DOI: 10.1002/aenm.201400678.
[10] a) L. Zhang, Z. Zhang, P. C. Redfern, L. A. Curtiss, K. Amine, *Energy Environ. Sci.* **2012**, *5*, 8204–8207; b) J. Huang, L. Cheng, R. S. Assary, P. Wang, Z. Xue, A. K. Burrell, L. A. Curtiss, L. Zhang, *Adv. Energy Mater.* **2015**, DOI: 10.1002/aenm.201401782.
[11] X. Wei, L. Li, Q. Luo, Z. Nie, W. Wang, B. Li, G. Xia, E. Miller, J. Chambers, Z. G. Yang, *J. Power Sources* **2012**, *218*, 39–45.
[12] W. Wang, S. Kim, B. Chen, Z. Nie, J. Zhang, G. Xia, L. Li, Z. Yang, *Energy Environ. Sci.* **2011**, *4*, 4068–4073.
[13] K. U. Schwenke, S. Meini, X. Wu, H. A. Gasteiger, M. Piana, *Phys. Chem. Chem. Phys.* **2013**, *15*, 11830–11839.
[14] a) V. S. Bryantsev, V. Giordani, W. Walker, M. Blanco, S. Zecevic, K. Sasaki, J. Uddin, D. Addison, G. V. Chase, *J. Phys. Chem. A* **2011**, *115*, 12399–12409; b) P. S. Engel, W. K. Lee, G. E. Marschke, H. J. Shine, *J. Org. Chem.* **1987**, *52*, 2813–2817.
[15] E. Nasybulin, W. Xu, M. H. Engelhard, Z. Nie, S. D. Burton, L. Cosimbescu, M. E. Gross, J. Zhang, *J. Phys. Chem. C* **2013**, *117*, 2635–2645.
[16] G. M. Robertson in *Comprehensive Organic Synthesis*, *Vol. 3* (Eds.: B. M. Trost, I. Fleming), Pergamon Press, Oxford, **1991**, pp. 563–611.

Received: February 13, 2015
Revised: March 18, 2015
Published online: April 20, 2015